J Physiol 588.18 (2010) pp 3403–3414

The Journal of Physiology

RAPID REPORT

The receptor subunits generating NMDA receptor mediated currents in oligodendrocytes

Valeria Burzomato, Guillaume Frugier, Isabel Pérez-Otaño, Josef T. Kittler and David Attwell

Department of Neuroscience, Physiology and Pharmacology, University College London, Gower Street, London WC1E 6BT, UK

NMDA receptors have been shown to contribute to glutamate-evoked currents in oligodendrocytes. Activation of these receptors damages myelin in ischaemia, in part because they are more weakly blocked by Mg^{2+} than are most neuronal NMDA receptors. This weak Mg^{2+} block was suggested to reflect an unusual subunit composition including the NR2C and NR3A subunits. Here we expressed NR1/NR2C and triplet NR1/NR2C/NR3A recombinant receptors in HEK cells and compared their currents with those of NMDA-evoked currents in rat cerebellar oligodendrocytes. NR1/NR2C/3A receptors were less blocked by 2 mM Mg^{2+} than were NR1/NR2C receptors (the remaining current was 30% and 18%, respectively, of that seen without added Mg^{2+}) and showed less channel noise, suggesting a smaller single channel conductance. NMDA-evoked currents in oligodendrocytes showed a Mg^{2+} block (to 32%) similar to that observed for NR1/NR2C/NR3A and significantly different from that for NR1/NR2C receptors. Co-immunoprecipitation revealed interactions between NR1, NR2C and NR3A subunits in a purified myelin preparation from rat brain. These data are consistent with NMDA-evoked currents in oligodendrocytes reflecting the activation of receptors containing NR1, NR2C and NR3A subunits.

(Resubmitted 25 June 2010; accepted after revision 19 July 2010; first published online 26 July 2010)

Corresponding author D. Attwell: Department of Neuroscience, Physiology and Pharmacology, University College London, Gower Street, London WC1E 6BT, UK. Email: d.attwell@ucl.ac.uk

Introduction

The myelin sheath insulates neuronal axons, thus speeding propagation of the action potential; however damage to the myelin is a characteristic of many severe CNS diseases. In brain and spinal cord trauma, stroke and multiple sclerosis the extracellular glutamate concentration in the CNS increases due to leakage from mechanically damaged cells, impaired or reversed uptake, increased glutamate synthesis and less breakdown, and possibly release from microglia. This overexcites glutamate receptors and triggers Ca^{2+} overload-driven death (excitotoxicity) of oligodendrocytes as well as neurons (Lipton & Rosenberg, 1994; Lee *et al.* 1999; Werner *et al.* 2001; Park *et al.* 2004; Káradóttir & Attwell, 2007).

Excitotoxicity in oligodendrocytes was originally thought to be mediated only by AMPA and kainate (KA) receptors. However, recent work suggests that there are NMDA receptors on the processes of oligodendrocytes, and that activation of these receptors in ischaemia damages the myelin (Ziak *et al.* 1998; Káradóttir *et al.* 2005; Salter & Fern, 2005; Micu *et al.* 2006), especially around the node of Ranvier (Fu *et al.* 2009), causing a loss of action potential propagation in the underlying axon (Bakiri *et al.* 2008; but see Tekkök *et al.* 2007). NMDA receptors may also contribute to damage to oligodendrocyte precursor cells in conditions leading to cerebral palsy (Káradóttir *et al.* 2008; Manning *et al.* 2008). In mature oligodendrocytes, block of AMPA/KA receptors was protective of oligodendrocyte somata (where these receptors are believed to be mainly located), but not sufficient to prevent damage to their processes during ischaemic insult (Salter & Fern, 2005; Micu *et al.* 2006).

Immunohistochemical and RT-PCR experiments indicate the presence of NR1, all NR2 (NR2A–D) and NR3A (but not NR3B) subunits in the optic nerve and cerebellar white matter (Káradóttir *et al.* 2005; Salter & Fern, 2005; Micu *et al.* 2006). However NMDA-evoked responses in white matter oligodendrocytes are insensitive to NR1/NR2A and NR1/NR2B receptor potentiators and inhibitors (Káradóttir *et al.* 2005), and myelin protection from ischaemic insult is provided by general NMDAR blockers, but not by specific NR1/NR2A and NR1/NR2B

V. Burzomato and G. Frugier contributed equally to this work.

DOI: 10.1113/jphysiol.2010.195503

blockers (Salter & Fern, 2005; Micu *et al.* 2006). Additionally, NMDA-evoked currents in oligodendrocytes show a Mg^{2+} block much weaker than is found for neuronal NMDA responses or for recombinant NR1/NR2A and NR1/NR2B receptors (Monyer *et al.* 1994; Kuner & Schoepfer, 1996; Ziak *et al.* 1998; Káradóttir *et al.* 2005), arguing against NR1/NR2A and NR1/NR2B as the composition of oligodendrocyte NMDARs. NR1, NR2C and NR3A were identified, by antibody labelling and quantification of mRNA levels, as the most abundant white matter NMDAR subunits; in particular NR2C was the most abundant of all NR2 subunits and NR3B was absent both at the mRNA and protein level (Káradóttir *et al.* 2005; Salter & Fern, 2005; but see Results). Additionally, partial colocalization of NR1, NR2C and NR3 was observed (Káradóttir *et al.* 2005). Collectively these observations led to the suggestion that oligodendrocyte NMDARs comprise NR1, NR2C and NR3A subunits (Káradóttir *et al.* 2005; Salter & Fern, 2005). However no direct functional evidence favouring this subunit composition is available, and both NR1/NR2C receptors and triplet NR1/NR2/NR3 receptors show a weak Mg^{2+} sensitivity (Monyer *et al.* 1994; Kuner & Schoepfer, 1996; Sasaki *et al.* 2002), which could be compatible with that observed for oligodendrocyte NMDA-evoked currents.

It is important to determine the composition of the NMDARs which damage oligodendrocytes, since these receptors could be a therapeutic target for myelin protection in white matter diseases, and their subunit composition is expected to determine their pharmacological properties. We therefore investigated which combination of the subunits suggested to be present in oligodendrocytes (NR1, NR2C and NR3A) might form oligodendrocyte NMDARs, by comparing NMDA-evoked currents in oligodendrocytes with NMDA responses from recombinantly expressed doublet NR1/NR2C and triplet NR1/NR2C/NR3A receptors.

Methods

Ethical information

Experiments were performed under the auspices of the UK Animals (Scientific Procedures) Act 1986, using humane (Schedule 1) killing of animals, for which no licence or ethical approval is required.

Cell culture

Human embryonic kidney (HEK) 293 cells were maintained at 37°C in 5% CO_2 in Dulbecco's modified Eagle's medium (DMEM) supplemented with 4 mM L-glutamine, 4.5 g l^{-1} D-glucose, 110 mg l^{-1} sodium pyruvate, 10% fetal calf serum, 100 U ml^{-1} penicillin G and 0.1 mg ml^{-1} streptomycin sulfate (all from Invitrogen, Carlsbad, CA, USA). The medium was changed every 2–3 days.

Cells were transfected with cDNAs encoding the rat NMDA receptor subunits NR1-1a (splice variants are described in Fig. 1) and NR2C (both subcloned into the pcDNA1 vector, Invitrogen), with or without NR3A tagged with enhanced green fluorescent protein (NR3A-EGFP, or untagged NR3A, see below) subcloned into the pCI-Neo vector (Promega Corp., Madison, WI, USA; all cloned in Dr Pérez-Otaño's lab). Transfection was either by calcium phosphate–DNA co-precipitation or electroporation. For expression of NR1-1a/NR2C receptors, the two subunits' cDNAs were transfected in a 1:1 ratio, together with a cDNA coding for EGFP to allow identification of transfected cells. For expression of NR1-1a/NR2C/NR3A receptors the NR1-1a, NR2C and NR3A-EGFP subunit cDNAs were transfected in ratios ranging from 1:1:1 to 1:1:10, with higher NR3A amounts being used in an attempt to minimize competing assembly of NR1-1a/NR2C receptors (although this apparently had no effect on the proportion of expressed receptors containing NR3A subunits, as judged by the Mg^{2+} block of the resulting currents: $P = 0.47$ from the t statistic for regression of Mg^{2+} block *versus* NR3A transfection ratio). We also co-transfected NR1-1a, NR2C, untagged NR3A and EGFP cDNAs, but no difference in the expression efficiency of NR1-1a/NR2C/NR3A receptors was noted between using tagged or untagged NR3A cDNA.

For calcium phosphate–DNA co-precipitation, HEK cells were plated 12–24 h before transfection onto poly-L-lysine coated 13 mm glass coverslips for electrophysiological measurements and into 100 mm culture dishes for biochemical analysis. The cDNA mix was added to a 340 mM $CaCl_2$ solution to produce a cDNA concentration of 0.022–0.030 μg μl^{-1}; this was then mixed with an equal volume of Hepes buffered saline (280 mM NaCl, 2.8 mM Na_2HPO_4, 50 mM Hepes; pH adjusted to 7.2 with NaOH) and immediately added to 35 mm Petri dishes, each one containing one coverslip plated with HEK cells and 1 ml growth medium. The total quantity of cDNA mix transfected per dish was 2.2–2.3 μg for NR1/NR2C receptor expression and 1.8–4.1 μg for NR1/NR2C/NR3A receptor expression. For electroporation, HEK cells were harvested, washed and resuspended in 0.5 ml Opti-MEM (Invitrogen), then the mix of cDNA (15.75–17.25 μg, 5–6 μl volume) was added in a cuvette and shocked in a Bio-Rad (Hercules, CA, USA) electroporator according to the manufacturer's specifications. Cells were then plated onto coverslips as previously described. No obvious difference in transfection efficiency was observed between the two methods. Blockers of the NMDAR glutamate and glycine binding sites, D-aminophosphono-valerate (D-AP5, 500 μM) and 7-chlorokynurenate (7-CK, 50 μM, or 5,7-dichlorokynurenate, 30–100 μM), were added to the

culture medium to avoid possible excitotoxic death due to activation of expressed NMDARs. After transfection, cells were cultured for 16–72 h before experiments.

Cerebellar slices

P12 rats were killed by cervical dislocation, and their cerebellum was quickly removed and sliced (thickness 225 μm) in ice-cold Krebs solution containing (mM) 124 NaCl, 26 $NaHCO_3$, 1 NaH_2PO_4, 2.5 KCl, 2 $MgCl_2$, 2.5 $CaCl_2$, 10 glucose, pH 7.4 when bubbled with 95% O_2–5% CO_2, and containing 1 mM sodium kynurenate to block glutamate receptors. Slices were stored in a chamber at room temperature (~23°C) filled with the same solution and recordings were made up to 8 h after slicing (using solutions defined below).

Electrophysiological recording

Both HEK cells and cells in the white matter of cerebellar slices were whole-cell patch-clamped with electrodes pulled from thick-walled borosilicate glass (GC150F-10, Harvard Apparatus, Holliston, MA, USA) to a resistance of 5–7 MΩ. The series resistance in whole-cell patch-clamp mode ranged from 5 to 31 MΩ and was compensated by up to 60%, giving a mean series resistance after compensation of 8 ± 1 MΩ (mean ± S.E.M.). Electrodes were filled with CsCl-based solutions. For HEK cells the solution contained (mM): 130 CsCl, 1 $CaCl_2$, 10 Hepes, 11 EGTA, 2 MgATP, 25 sucrose, pH set to 7.3 with CsOH. When recording from cells transfected with NR1-1a, NR2C and NR3A (tagged or untagged) the frequency of responding cells was quite low, so in some experiments we added 50 μM dynamin inhibitory peptide to the electrode solution to check whether dynamin-dependent internalization was the cause of such low surface expression of receptors. However we observed no difference in the frequency of responding cells with the addition of this blocker.

For white matter cells the electrode-filling solution contained (in mM): 130 CsCl, 4 NaCl, 0.5 $CaCl_2$, 10 Hepes, 10 BAPTA, 2 MgATP, 0.5 Na_2GTP, 2 K-Lucifer yellow, pH set to 7.3 with CsOH. The Lucifer yellow allowed visualization of the cells' morphology.

The superfusion solution (bubbled with 100% O_2 and at room temperature, ~23°C) contained (in mM): for HEK cells, 140 NaCl, 2.5 KCl, 2.5 $CaCl_2$, 10 Hepes, 15 glucose, 15 sucrose, pH set to 7.4 with NaOH; for slices, 144 NaCl, 2.5 KCl, 2.5 $CaCl_2$, 10 Hepes, 1 NaH_2PO_4, 10 glucose, pH set to 7.4 with NaOH. For magnesium block experiments 2 mM $MgCl_2$ was added to the superfusion solution. Drugs (NMDA 60 μM, glycine 100 μM) were diluted in the superfusion solution. For experiments on HEK cells, semi-fast application of drugs was achieved with a combination of bath perfusion and a home-made U-tube system, consisting of a U-shaped capillary with a small hole at the apex. One branch of the U-tube was connected to a vacuum pump, and the other to the drug solution reservoir. The U-tube was placed close to the patched cell and when drug application was needed the connection to the vacuum pump was interrupted and a fast stream of solution was expelled from the hole onto the cell, providing solution exchange times of <0.6 s (not fast enough to analyse the kinetics of onset of the response to NMDA). On re-connecting the vacuum pump, the background bath perfusion removes the applied drugs with a time constant of less than 5 s. NMDA was applied once every 2 min (122 ± 6 s, $n = 56$), and at this repetition rate there was negligible desensitization, and a negligible reduction in the response amplitude by residual Mg^{2+} when NMDA was applied in 0 Mg^{2+} after a prior application in 2 mM Mg^{2+} (when applying NMDA 3 times sequentially in 0, 2 and then again in 0 mM Mg^{2+}, the response to the last application was $95 \pm 5\%$ ($n = 22$) of the first response (not significantly different, $P = 0.33$). U-tube drug application could not be used for slices, as the fast flow would displace the slice and cause seal loss, so drugs were bath-applied to slices.

Glycine was pre-applied before NMDA for experiments on HEK cells transfected with the NR1-1a, NR2C and NR3A subunits. This allowed us to distinguish the NMDA-evoked current from a possibly present glycine-evoked current mediated by NR1/NR3A glycine receptors (Chatterton *et al.* 2002), which could assemble in these transfection conditions. In experiments on NR1-1a/NR2C transfected HEK cells and slices, glycine was also routinely pre-applied (together with 5 μM strychnine for experiments on slices, in order to avoid glycine receptor activation). We also recorded from some cells without glycine pre-application and found that applying glycine and NMDA together did not obviously change the time course of the NMDA responses, suggesting that the solution exchange time of our drug application was slower than the time needed for glycine binding (or that contaminant glycine in the superfusion solution was adequate to activate the receptor).

Statistics

Data are presented as mean ± S.E.M. Heteroscedastic *t* tests (allowing unequal variance) were used to assess significance.

Myelin preparation

Purified myelin was prepared as previously described (Norton & Poduslo, 1973). Briefly, brains from adult Sprague–Dawley rats were homogenized in a 0.32 M

sucrose solution. The homogenate was layered over a 0.85 M sucrose solution, and centrifuged at 17,800 g for 30 min (the purification step). After osmotic shocks in deionised water, and one or two repeats of the purification step, the purified myelin was retrieved at the interface of the 0.32 M and 0.85 M sucrose solutions. Finally, the myelin was washed in cold deionised water, and pelleted by centrifugation at 10,600 g for 10 min. Purity of this preparation was assessed by Western blotting using antibodies directed against neuronal (NeuN, mouse monoclonal, Millipore, Billerica, MA, USA), astrocytic (Aldh1L1, mouse monoclonal, NeuroMab, Davis, CA, USA) and oligodendroglial (MOG, rabbit polycolonal, Sigma) markers as described in the main text.

Immunoprecipitation

Proteins in transfected HEK cells or myelin preparations were solubilized for 2 h in buffer containing 50 mM Tris pH 7.5, 1% Triton X-100, 0.1% SDS, 150 mM NaCl, 1 mM EDTA and a cocktail of proteases inhibitors (1 mM PMSF, aprotinin 10 μg ml^{-1}, leupeptin 10 μg ml^{-1}, pepstatin 10 μg ml^{-1}). Cell debris and membranes were removed by centrifugation at 20,800 g for 30 min. The supernatant was incubated for 1 h with 15 μl of protein-A or -G sepharose beads (Generon, Maidenhead, UK), depending on the antibody used for the immunoprecipitation, and centrifuged at 425 g for 5 min. The clarified supernatant was then incubated overnight at 4°C with 10 μg of goat polyclonal anti-NR2C (Santa Cruz Biotechnology, Inc., Santa Cruz, CA, USA), 5 μg of mouse anti-GFP or rabbit polyclonal anti-NR3A (Millipore) antibodies, or with 10 μg of their corresponding control IgG (Santa Cruz), and then for 1 h with protein-A or -G sepharose beads. The resin was finally washed thrice in solubilisation buffer and twice with the same buffer containing 500 mM NaCl.

Western blotting

The beads were resuspended in 15 μl of loading buffer, and separated by 10% SDS-PAGE. Proteins were then transferred onto nitrocellulose membrane (Amersham Hybond-ECL, GE Healthcare, Little Chalfont, UK). The membranes were blocked in phosphate-buffered saline (PBS) supplemented with 0.5% Tween (National Diagnostics, Atlanta, GA, USA) and 4% milk. Immunoblotting was performed at 4°C under agitation overnight with the appropriate antibodies: goat polyclonal anti-NR2C antibody (1:4000; Santa Cruz), rabbit polyclonal anti-NR3A (1:1000; Millipore) and mouse monoclonal anti-NR1 (1:1000; BD Biosciences, Franklin Lakes, NJ, USA) or anti-GFP (1:1000; Roche). The following HRP-conjugated secondary antibodies were applied to the membranes for 1 h at room temperature: donkey anti-goat (1:10 000; Santa-Cruz), anti-mouse (1:5000; Rockland Immunochemicals Inc., Gilbertsville, PA, USA) and anti-rabbit (1:5000; Rockland). Finally, proteins were detected by chemiluminescence using ECL reagent (Thermo Fisher Scientific Inc., Rockford, IL, USA). Different antigens were detected consecutively on the same blot after stripping in a buffer containing 10% SDS and 350 mM β-mercaptoethanol in water, and blocking the membranes again before applying another primary antibody.

RT-PCR

Total RNA was extracted from two adult rat optic nerves using TRI reagent (Sigma) according to the manufacturer's specifications. The reverse transcription reaction was run at 50°C for 1 h in a 20 μl final volume containing 200 units of Superscript III RT (Invitrogen), 250 ng random primers (Promega), 500 μM dNTP mix (Fermentas International Inc., Burlington, ON, Canada), 5 mM dithiothreitol and 40 units of RNasin plus RNase inhibitor (Promega). Finally, the reverse transcriptase was heat-inactivated at 70°C for 15 min. The PCR reactions were run in a final 50 μl volume containing 2 μl of single-strand cDNA, 5 units of Taq polymerase and 5 μl of polymerase buffer (New England Biolabs, Inc., Ipswich, MA, USA), 1.5 mM $MgCl_2$, 500 μM dNTP mix (Fermentas), 200 nM of each primer (Eurofins MWG Operon, Ebersberg, Germany) and 37 μl autoclaved water. The amplification of the reverse transcribed RNA was run under the following conditions: 94°C for 3 min, then 35 cycles of 50 s at 94°C, 50 s at 55°C and 1 min 45 s at 72°C, then a final step at 72°C for 5 min. The primers used to detect all known NMDA subunits were described previously (Edwards *et al.* 2004, and see Fig. 1*A* and *B*). PCR products were resolved by agarose gel electrophoresis and visualised with ethidium bromide). Negative controls run by omitting the reverse-transcriptase, the mRNA or the cDNA did not show any amplification in the experiments.

Results

NMDA receptors subunit are expressed in the white matter

We assessed which NMDA subunits are expressed in central white matter, by applying RT-PCR to the adult rat optic nerve, using primers designed to amplify all known NMDAR subunits and their splice variants (Edwards *et al.* 2004). Various N- and C-terminal variants of NMDA receptor NR1 subunits are known to exist (Fig. 1*A*), which were identified using the primer combinations in Fig. 1*B*.

This revealed the presence of the NR1-1, NR1-2 and NR1-4 (but not NR1-3) C-terminal variants, and both the 'a' and 'b' N-terminus splice variants (Fig. 1*B*). Similarly all NR2 (NR2A–D, Fig. 1*C*), and both NR3 (NR3A and NR3B) subunits (Fig. 1*D*) were identified. In contrast, Salter & Fern (2005) found little NR3B both at the mRNA level and using antibody labelling (this difference might reflect their studying mouse rather than rat tissue).

As described in the Introduction, other observations limit the number of subunit combinations which are most relevant to be investigated electrophysiologically. Previous pharmacological data show that receptors made of NR1/NR2A and NR1/NR2B subunit combinations do not

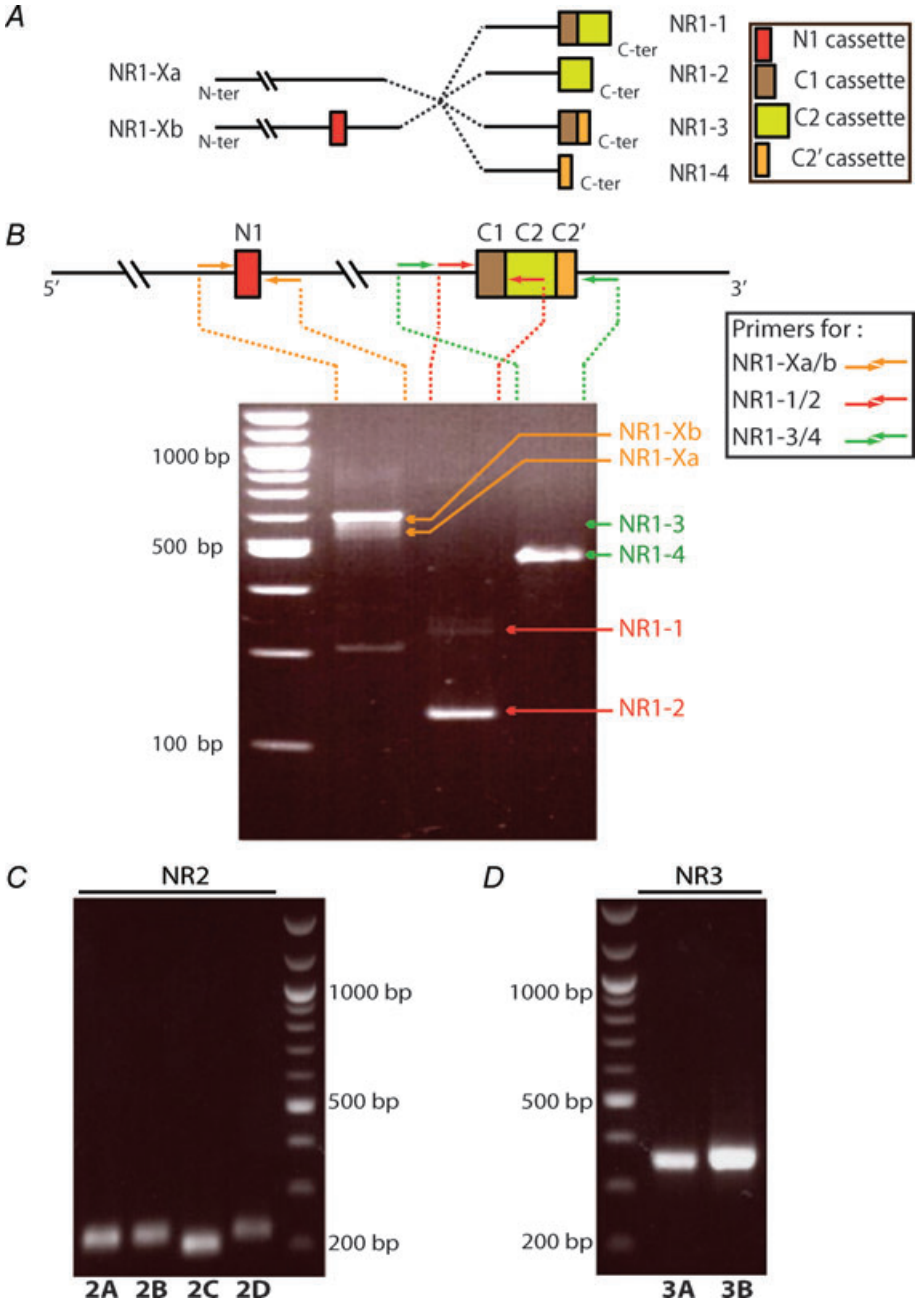

Figure 1. NMDA receptor subunits present in the optic nerve
A, different N-terminal (a and b) and C-terminal (1 to 4) variants of the NR1 subunit. *B*, primers used to identify the different NR1 variants, and ethidium bromide stained agarose gel showing RT-PCR products for the mRNA for the different variants from adult rat optic nerve. *C*, agarose gel showing RT-PCR products for the different NR2 subunits. *D*, agarose gel showing RT-PCR products for the different NR3 subunits.

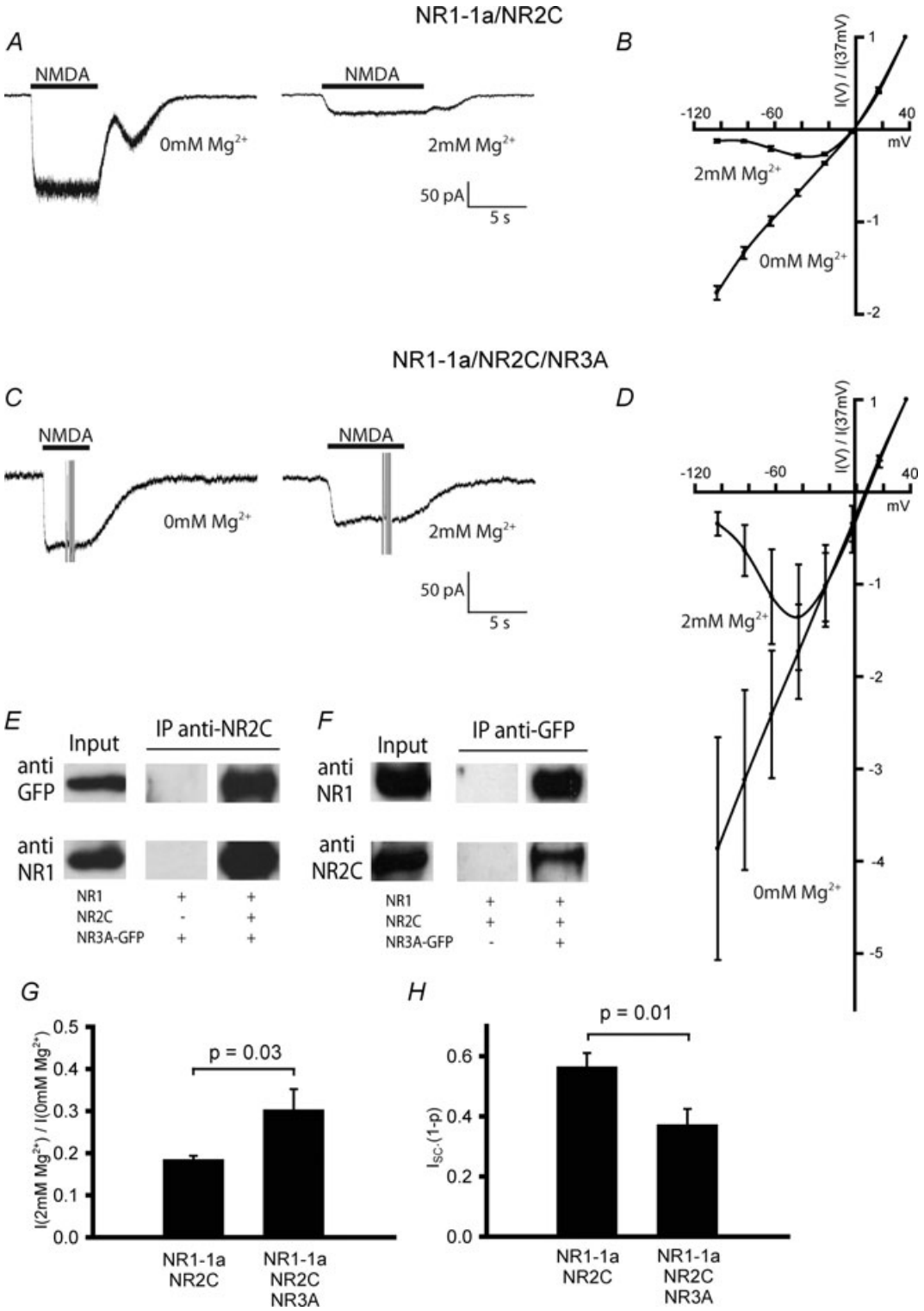

Figure 2. The properties of recombinant NR1-1a/NR2C and NR1-1a/NR2C/NR3A receptors
A, specimen responses at −63 mV of a HEK cell expressing NR1-1a and NR2C subunits to 60 μM NMDA in 0 and 2 mM Mg^{2+} solution (the transient inward current at the end of the NMDA application reflects swirling of the solution in the perfusion system, and should be ignored). The decrease in baseline (pre-NMDA) current noise in this record and in panel *C* reflects a decrease in seal conductance produced by the increase in [Mg^{2+}] (Formenti & De Simoni, 2000; Priel *et al.* 2007). *B*, mean *I–V* relation of the NMDA-evoked currents as in *A*, in 8 cells. Non-linearity in the nominally 0 mM Mg^{2+} plot may reflect weak block at negative potentials by trace Mg^{2+}

mediate NMDA-evoked currents and ischaemic damage to oligodendrocytes, and that the Mg^{2+} sensitivity of these receptors is much higher than is seen for oligodendrocyte NMDA currents. Káradóttir *et al.* (2005) found that 2 mM Mg^{2+} reduced the oligodendrocyte NMDA response at −63 mV to ∼30% of its value in 0 mM Mg^{2+}. The oocyte expression data of Kuner & Schoepfer (1996) predict that the residual current in 2 mM Mg^{2+} for NR1/NR2A and NR1/NR2B receptors would be 1.9% and 1.4% of that in 0 mM Mg^{2+}, respectively, while for NR1/NR2C and NR1/NR2D receptors it would be 5.8% and 4.1%. However, for receptors expressed in mammalian cells, where the different membrane lipid composition could alter the Mg^{2+} block, data of Monyer *et al.* (1994) predict a weaker block for NR1/NR2C and NR1/NR2D receptors, with a residual current of 25% and 33%, respectively (using the Hill coefficient for Mg^{2+} block of 0.93 from Kuner & Schoepfer (1996)). Inclusion of an NR3 subunit with NR1 and NR2 subunits may either greatly decrease Mg^{2+} block (using NR3A: Sasaki *et al.* 2002) or have no effect on the block (NR3B: Yamakura *et al.* 2005). Thus, the observed weak Mg^{2+} block in oligodendrocytes *in situ* is compatible with the receptors being composed of NR1 together with NR2C or NR2D (doublet receptors) or being triplet receptors comprising NR1, an NR2 subunit and NR3A.

To evaluate whether receptors of the NR1/NR2 or NR1/NR2/NR3 type generate oligodendrocyte NMDA responses, we studied doublet (NR1/NR2) or triplet (NR1/NR2/NR3) receptors containing the NR2C and NR3A subunits, recombinantly expressed in HEK cells. The NR2C and NR3A subunits were chosen (as opposed to NR2D and NR3B) because of previous indications of their abundance and colocalization in the myelin (Káradóttir *et al.* 2005; Salter & Fern, 2005; see Introduction), and because introduction of the NR3B subunit to NR1/NR2 receptors has been reported not to reduce their Mg^{2+} block (Yamakura *et al.* 2005).

Among the six NR1 isoforms revealed in our RT-PCR analysis, we restricted our investigation to recombinant receptors incorporating NR1-1a, the splice variant routinely used in studies of recombinant NMDARs expressed in oocytes and mammalian cell lines (Kuner & Schoepfer, 1996; Pérez-Otaño *et al.* 2001; Sasaki *et al.* 2002; Matsuda *et al.* 2003). Incorporation of different NR1 splice variants into NMDARs influences some of the receptors' kinetic and pharmacological properties, such as inhibition by protons and Zn^{2+} and potentiation by polyamines (reviewed by Dingledine *et al.* 1999). However, consistent with these splice variants altering only the N- and C-terminals of the receptors and not the transmembrane region, there is no evidence of these variants influencing the receptor's Mg^{2+} sensitivity, the key feature which distinguishes oligodendrocyte NMDA receptors from those in neurons.

Incorporation of the NR3A subunit decreases the Mg^{2+} block and current noise of recombinant NMDA receptors containing NR1-1a and NR2C

To quantify the fraction of the NMDA-evoked current that was blocked by Mg^{2+} in recombinant NR1/NR2C and NR1/NR2C/NR3A receptors, the current response in 2 mM Mg^{2+} was divided by the average of two bracketing responses in nominally 0 Mg^{2+}.

Figure 2*A* shows specimen currents elicited at −63 mV by application of 60 μM NMDA to NR1-1a/NR2C receptors in 0 and 2 mM Mg^{2+}. These currents showed a large noise increase on drug application, and the response in 2 mM Mg^{2+} was 18 ± 1% of the response in 0 Mg^{2+} ($n = 8$), compatible with the range of values previously reported for these receptors (Kutsuwada *et al.* 1992; Monyer *et al.* 1992; Ishii *et al.* 1993; Monyer *et al.* 1994; Kuner & Schoepfer, 1996). When we transfected HEK cells with NR1-1a, NR2C and NR3A–EGFP, the proportion of cells responding to NMDA decreased considerably, compared to cells transfected with NR1 and NR2C only. However, we demonstrated by co-immunoprecipitation experiments that NR3A–EGFP could interact with NR1, and also with NR2C, in HEK cells, as is necessary for the formation of triplet NMDARs. We were able to co-immunoprecipitate NR3A–EGFP and NR1 using an antibody directed against NR2C (Fig. 2*E*). Alternatively,

in the solution. *C*, specimen responses at −63 mV of a HEK cell expressing NR1-1a, NR2C and NR3A-EGFP subunits to 60 μM NMDA in 0 and 2 mM Mg^{2+} solution. The vertical lines on the trace during drug application are due to voltage steps applied to obtain an *I–V* relation. *D*, mean *I–V* relation of the NMDA-evoked currents as in *C*, in 4 cells. Same vertical scale as in *B*. *E*, Western blot showing immunoprecipitation (IP) of lysate from HEK cells expressing NR1-1a, NR2C and NR3A–EGFP subunits, with antibody against NR2C, probed with antibodies against EGFP (= NR3A) and NR1. This experiment was repeated 3 times. *F*, Western blot showing immunoprecipitation (IP) of lysate from HEK cells expressing NR1-1a, NR2C and NR3A–EGFP subunits, with antibody against EGFP (= NR3), probed with antibodies against NR2C and NR1. This experiment was repeated 3 times. *G*, mean value for NMDA-evoked current in 2 mM Mg^{2+} relative to that in 0 mM Mg^{2+} for 8 cells expressing NR1-1a and NR2C subunits and 16 cells expressing NR1-1a, NR2C and NR3A subunits. All cells were clamped at −63 mV. *H*, ratio of current variance to mean current (= single channel current × (1 − open probability)) for NMDA-evoked responses in cells transfected with NR1-1a, NR2C ($n = 8$ cells) or with NR1, NR2C and NR3A subunits ($n = 16$).

NR1 and NR2C could be pulled down with NR3A–EGFP using an antibody directed against GFP (Fig. 2*F*). It is possible, therefore, that although NR1/NR2C/NR3A receptors are formed, in many cells they are not inserted into the surface membrane in sufficient numbers to generate a detectable current.

NMDA-evoked currents in 0 and 2 mM Mg^{2+} recorded from a representative cell transfected with NR1-1a, NR2C and NR3A are shown in Fig. 2*C*. In these cells, the response to NMDA in 2 mM Mg^{2+} was $30 \pm 5\%$ of the control in 0 Mg^{2+}, significantly larger than the value observed for NR1-1a/NR2C receptors (Fig. 2*G*, $n = 16$ for NR1-1a, NR2C and NR3A expressing cells; $n = 8$ for NR1-1a and NR2C expressing cells). In addition, the *I–V* relation for the NMDA-evoked current in 2 mM Mg^{2+} in these cells showed a significantly larger current (normalized to the current at +37 mV where there is negligible Mg^{2+} block) at voltages more negative than −20 mV than did the *I–V* relation for the NMDA-evoked current in cells expressing NR1/NR2C receptors ($P < 0.03$ for all voltages negative to −20 mV, 8 cells for NR1/NR2C and 4 cells for NR1/NR2C/NR3A, Fig. 2*B* and *D*).

Cells transfected with NR1-1a, NR2C and NR3A-EGFP showed a smaller increase of current noise evoked by NMDA application than did cells transfected with NR1-1a and NR2C (Fig. 2*A* and *C*). This is expected if, like triplet NR1/NR2A/NR3A or NR1/NR2B/NR3A receptors (Das *et al.* 1998; Pérez-Otaño *et al.* 2001; Sasaki *et al.* 2002), NR1/NR2C/NR3A receptors have a smaller single channel conductance than NR1/NR2C receptors, which is expected to lower the noise produced by channel opening and closing.

A current noise parameter, reflecting the open channel current of the receptors, was obtained by taking the ratio of the NMDA-evoked current variance to the NMDA-evoked mean current in zero-Mg^{2+} solution. In the absence of series resistance filtering this parameter is equal to the single channel current, I_{sc}, multiplied by (1-p), where p is the channel open probability (Neher & Stevens, 1977). Whole-cell traces were 8-pole Bessel low-pass filtered at 500 Hz (defined by our sampling rate of 1 kHz) and high-pass filtered at 1 Hz. The noise power spectra of two trace sections of equal length (>1 s), one before (control) and one during NMDA application, were calculated (with Clampfit software, Molecular Devices, Sunnyvale, CA, USA) and subtracted. To improve the estimate of the variance, by extrapolating to zero and infinite frequency the noise components detected in the frequency range imposed by the high and low pass filters, the resulting spectrum of the NMDA-evoked noise was then fitted with a Lorentzian curve in 24 cells or, in two cells to improve the fit, the sum of two Lorentzian curves:

$$G(f) = G_0 / \left[1 + (f/f_c)^2\right]$$

where G_0 is the zero-frequency asymptote and f_c the half-power frequency of one Lorentzian component. This gives an estimate for the variance of the NMDA-evoked current of

$$\text{variance} = (\pi/2) \times \sum_i G_{0i} f_{ci}$$

so that, for a low open channel probability p, the single channel current (I_{sc}) is estimated as:

$$\text{variance}/(\text{mean current}) = I_{sc}(1-p) = (\pi/2) \times \sum_i (G_{0i} f_{ci})/I_{NMDA}$$

where G_{oi} and f_{ci} are the parameters obtained from the fitted Lorentzians and I_{NMDA} is the mean NMDA-induced current. In the whole-cell configuration the combination of the cell capacitance (C) and the electrode series resistance (R_S) produces a low-pass filter of cut-off frequency $f_{Rs} = 1/2\pi R_S C$. For each recording, R_s and C were estimated (by fitting the transient current elicited by a voltage step: Tessier-Lavigne *et al.* 1988) and the corresponding cut-off frequency was calculated. We accepted for further analysis only recordings with $f_{Rs} > 500$ Hz, for which the loss of variance caused by the $R_S C$ filtering was <7%.

Derived in this way, the mean value of the noise parameter (variance of NMDA-evoked current)/(mean NMDA-evoked current) for NR1/NR2C receptors was 0.56 ± 0.05 pA (at −63 mV, $n = 8$, Fig. 2*H*). For a reversal potential of 0 mV (Fig. 2*B*), if all the channel noise is recorded and the channel open probability is low (∼0.01: Dravid *et al.* 2008), this would correspond to a single channel conductance of 0.56 pA/0.063 V or ∼9 pS, which is considerably less than the conductance levels of 20 and 33 pS measured (also at 23°C) in cerebellar granule cells in 1 mM $[Ca^{2+}]_o$ (Farrant *et al.* 1994). This may largely reflect the fact that our recordings were in 2.5 mM $[Ca^{2+}]_o$, since Dravid *et al.* (2008) found that the conductances of these substates are decreased from 48 and 57 pS in 0 mM $[Ca^{2+}]_o$ (at 23°C) to 28 and 45 pS in 0.5 mM $[Ca^{2+}]_o$. Combining the data from Farrant *et al.* (1994) and Dravid *et al.* (2008), and extrapolating the Ca^{2+} dependence thus obtained (assuming a $1/(1+[Ca^{2+}]_o/K_m)$ dependence, with K_m constant, for the reduction of conductance by Ca^{2+}), predicts conductance states of 10.5 and 21.5 pS at 2.5 mM $[Ca^{2+}]_o$, the lower of which is close to the 9 pS value derived from the noise. However some noise variance on the time scale of channel opening (0.5–0.8 ms in 0.5–1 mM $[Ca^{2+}]_o$: Farrant *et al.* 1994; Dravid *et al.* 2008) may also be lost by sampling at 1 kHz and subsequent filtering at 500 Hz.

The mean single channel current estimated similarly from the variance and mean of the NMDA-evoked current in cells transfected with NR1-1a, NR2C and

NR3A was 0.37 ± 0.05 pA ($n = 16$), which is significantly less than the value obtained for NR1/NR2C receptors (Fig. 2*H*). Assuming no change in the fraction of noise lost by filtering and that the open probability is low, this indicates that the single channel conductance of the triplet channels is lower, as observed previously when an NR3A subunit was incorporated into NR1/NR2A receptors (Das *et al.* 1998; Pérez-Otaño *et al.* 2001; Sasaki *et al.* 2002).

The Mg^{2+} block of NMDA currents in mature oligodendrocytes is similar to the value for NR1-1a/NR2C/NR3A receptors

We recorded currents elicited by application of NMDA to cerebellar white matter oligodendrocytes patch-clamped at −63 mV in the whole-cell configuration. These cells were identified by their characteristic morphology (many long processes parallel to each other and to the direction of the axons: Fig. 3*A*), confirmed by antibody labelling for

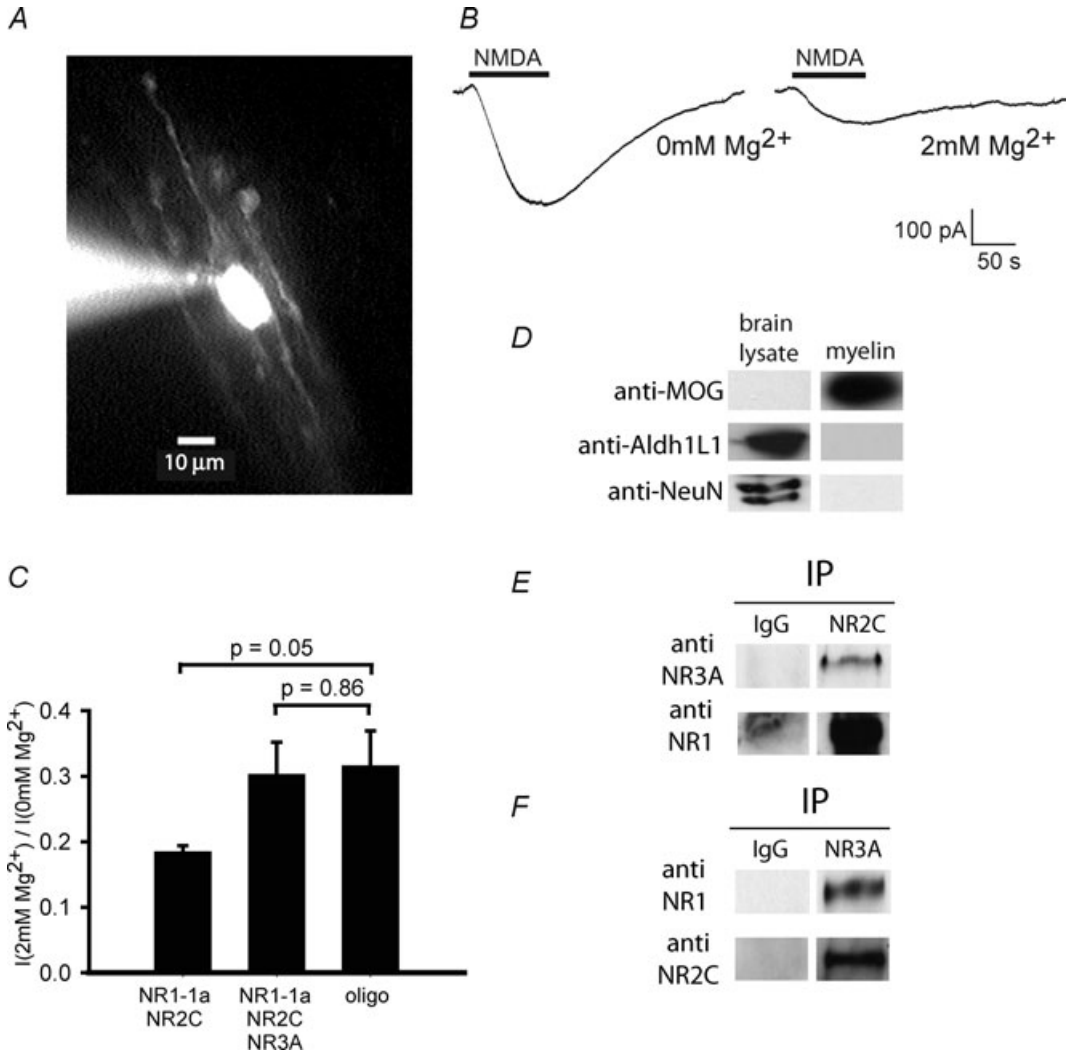

Figure 3. Comparison of NMDA-evoked currents in oligodendrocytes with those generated by recombinant receptors

A, Lucifer yellow filled oligodendrocyte in the white matter of the cerebellum. *B*, specimen currents evoked in an oligodendrocyte at −63 mV by 60 μM NMDA in 0 and 2 mM Mg^{2+}. *C*, mean value for NMDA-evoked current in 2 mM Mg^{2+} relative to that in 0 mM Mg^{2+} for 7 oligodendrocytes, compared with values from Fig. 2*G* for cells expressing NR1-1a and NR2C subunits or NR1-1a, NR2C and NR3A subunits. *D*, assessment of purity of myelin preparation, using antibodies against myelin/oligodendrocyte glycoprotein (MOG) to label myelin, aldehyde dehydrogenase 1 type L1 (Aldh1L1) to label astrocytes (Cahoy *et al.* 2008), and NeuN to label neurons (the antibody recognises two isoforms with different molecular weights). *E*, Western blot showing immunoprecipitation (IP) of myelin preparation using antibody to NR2C probed with antibodies to NR3A and to NR1. This experiment was repeated twice. *F*, Western blot showing immunoprecipitation (IP) of myelin preparation using antibody to NR3A probed with antibodies to NR1 and to NR2C. This experiment was repeated twice.

myelin basic protein in some cells (Káradóttir *et al.* 2005). In nominally 0 mM Mg^{2+} oligodendrocytes showed a mean response to 60 μM NMDA of 300 ± 100 pA ($n = 7$), which was reduced to 32 ± 5% of this control value in 2 mM Mg^{2+} (Fig. 3*B*). This value, which is similar to that found by Káradóttir *et al.* (2005), is not significantly different from the value we observed for NR1-1a/NR2C/NR3A receptors, but is significantly larger than the value for NR1-1a/NR2C receptors (Fig. 3*C*).

We did not analyse the noise of the NMDA-evoked current in oligodendrocytes as we did for recombinant receptors, because these cells have a capacitance about 10 times higher than HEK cells. This, together with the pipette series resistance, filters the signal with a low-pass cut-off frequency much lower than the limit we accepted for HEK cells (500 Hz).

NR1, NR2C and NR3A can interact in the myelin

To support the idea that NR1/NR2C/NR3A receptors might generate oligodendrocyte NMDA responses, we tested for interaction of these subunits in the white matter. We carried out co-immunoprecipitation experiments on myelin preparations purified from adult rat brains (see Methods) which contained no detectable astrocyte or neuronal contamination (Fig. 3*D*). Using antibodies to NR2C and NR3A, we were able to pull down, respectively, NR1 and NR3A (Fig. 3*E*), and NR1 and NR2C (Fig. 3*F*). In experiments where control IgGs were used instead of specific antibodies, co-immunoprecipitation was abolished (Fig. 3*E* and *F*).

The fact that NR3A is found interacting with NR1, and also with NR2C, is consistent with the presence of receptor complexes containing all three NR1, NR2C and NR3A subunits in the myelin, where oligodendrocyte NMDA receptors have previously been reported (Káradóttir *et al.* 2005; Salter & Fern, 2005; Micu *et al.* 2006).

Discussion

The data presented in this paper advance our understanding of the influence of NR3 subunits on NMDA receptor function and give insight into the receptor subunits that may contribute to generating NMDA-evoked currents in oligodendrocytes.

Previous work showed that including an NR3 subunit with NR1 and NR2A or 2B subunits either greatly decreased Mg^{2+} block (using NR3A: Sasaki *et al.* 2002) or had no effect on the block (NR3B: Yamakura *et al.* 2005), although it is not clear whether triplet receptors were actually formed at the surface membrane in the latter paper. Incorporating an NR3A subunit with NR1 and NR2A also reduced the conductance of NMDA receptors (Das *et al.* 1998; Pérez-Otaño *et al.* 2001; Sasaki *et al.* 2002). Our experiments extend to receptors including NR1 and the more weakly Mg^{2+} blocked subunit NR2C the fact that including an NR3A subunit reduces the Mg^{2+} block still further (the NMDA-evoked current in 2 mM Mg^{2+} as a percentage of that in 0 mM Mg^{2+} was 30% for NR1/NR2C/NR3A receptors *versus* 18% for NR1/NR2C receptors: Fig. 2*G*). Furthermore, the smaller current noise associated with the responses generated by NR1/NR2C/NR3A receptors than by NR1/NR2C receptors (Fig. 2*H*) is consistent with a decrease in single channel conductance. Since we cannot exclude the formation of some NR1/NR2C receptors when expressing all three subunits, it is possible that the Mg^{2+} block and single channel conductance for NR1/NR2C/NR3A receptors are even smaller, relative to those for NR1/NR2C receptors, than is indicated by these data.

Oligodendrocytes in brain slices show NMDA-evoked currents that have tentatively been attributed, on the basis of immunocytochemical and pharmacological studies, to receptors containing NR1, NR2C and NR3 subunits being present in the oligodendrocyte membrane (Ziak *et al.* 1998; Káradóttir *et al.* 2005; Salter & Fern, 2005; Micu *et al.* 2006). Interestingly, expression of mRNA for NR3A and NR1 apparently decreases with the development of oligodendrocyte lineage cells, to reach very low levels in mature cells (Cahoy *et al.* 2008). Nevertheless, consistent with NR1/NR2C/NR3A NMDA receptors being present in the oligodendrocytes, NMDA receptor subunits are expressed in the white matter (Fig. 1), the NR3A subunit can bind to NR1 and to NR2C (Fig. 3*D–F*), and NMDA-evoked currents in oligodendrocytes are unaffected when action potentials (which might generate a current in oligodendrocytes by releasing K^+) were blocked by TTX (Káradóttir *et al.* 2005), and were still present when synaptic transmission was blocked using Ca^{2+}-free solution or when K^+ influx was inhibited with Ba^{2+} (Ziak *et al.* 1998). However no direct evidence for the subunit combination generating oligodendrocyte NMDA responses has been presented so far.

As noted above, the Mg^{2+} block observed for oligodendrocyte NMDA currents is in principle compatible with the block previously reported for recombinant NR1/NR2C, NR1/NR2D (but NR2D is weakly expressed in the white matter) or triplet NR1/NR2/NR3A receptors (Monyer *et al.* 1994; Kuner & Schoepfer, 1996; Sasaki *et al.* 2002). NMDA-evoked currents in 2 mM Mg^{2+} in oligodendrocytes were 32 ± 5% of the size of those seen in 0 mM Mg^{2+}, similar to the value found for NR1/NR2C/NR3A receptors but significantly larger than that found for NR1/NR2C receptors. These observations are consistent with the hypothesis that triplet NR1/NR2C/NR3A receptors are mainly responsible for generating NMDA-evoked currents in cerebellar oligodendrocytes.

We cannot be certain that this conclusion will generalise to all brain areas. However, to date, no indication of a different composition of NMDA receptors in different CNS white matter areas has been reported. The unusual pharmacological properties and weak Mg^{2+} block, which distinguish oligodendroglial from neuronal NMDA receptor currents, have been observed for rodent oligodendrocytes at different stages of maturation and located in different CNS areas. Expression of NR1, NR2C and NR3 subunits has been reported in the white matter of the P7–14 cerebellum (Káradóttir *et al.* 2005) and in the P7–P13 and adult optic nerve (Micu *et al.* 2006; Salter & Fern, 2005). Insensitivity of NMDA-evoked currents to NR1/NR2A and NR1/NR2B potentiators and inhibitors is reported for white matter oligodendrocytes in P7–14 cerebellar slices (Káradóttir *et al.* 2005), and protection of myelin from ischaemic insult has been observed with general NMDA receptor blockers but not with specific NR1/NR2A and NR1/NR2B blockers in the P7–13 and adult optic nerve (Micu *et al.* 2006; Salter & Fern 2005). A weak sensitivity to Mg^{2+} has been observed for NMDA receptor currents in white matter oligodenrocyte lineage cells at different stages of maturation (precursor, pre-myelinating and mature myelinating oligodendrocytes) in P7–14 cerebellar slices (Káradóttir *et al.* 2005) and in oligodendrocytes in spinal cord slices (Ziak *et al.* 1998). Thus, on the basis of these observations, the presence of NMDA receptors of an unusual subunit composition, which underlies their distinctive properties, seems to be a general property of oligodendrocytes, irrespective of their location and stage of development.

In ischaemic conditions an intracellular Ca^{2+} rise, and subsequent damage causing a loss of action potential propagation, has been observed in the oligodendrocytes' myelinating processes, which is prevented by NMDAR blockers (Salter & Fern, 2005; Micu *et al.* 2006; Bakiri *et al.* 2008). These receptors could therefore be a therapeutic target for myelin protection in pathologies involving excitotoxic stress, such as spinal cord injury and multiple sclerosis. The presence in the white matter of NMDARs including the NR3A subunit, which may have a pharmacological profile different from that of neuronal NMDARs, could allow the development of selective NMDA blockers conferring myelin protection without interfering with neuronal NMDA activity.

References

Bakiri Y, Hamilton NB, Káradóttir R & Attwell D (2008). Testing NMDA receptor block as a therapeutic strategy for reducing ischaemic damage to CNS white matter. *Glia* **56**, 233–240.

Cahoy JD, Emery B, Kaushal A, Foo LC, Zamanian JL, Christopherson KS, Xing Y, Lubischer JL, Krieg PA, Krupenko SA, Thompson WJ & Barres BA (2008). A transcriptome database for astrocytes, neurons, and oligodendrocytes: a new resource for understanding brain development and function. *J Neurosci* **28**, 264–278.

Chatterton JE, Awobuluyi M, Premkumar LS, Takahashi H, Talantova M, Shin Y, Cui J, Tu S, Sevarino KA, Nakanishi N, Tong G, Lipton SA & Zhang D (2002). Excitatory glycine receptors containing the NR3 family of NMDA receptor subunits. *Nature* **415**, 793–798.

Das S, Sasaki YF, Rothe T, Premkumar LS, Takasu M, Crandall JE, Dikkes P, Conner DA, Rayudu PV, Cheung W, Chen HS, Lipton SA & Nakanishi N (1998). Increased NMDA current and spine density in mice lacking the NMDA receptor subunit NR3A. *Nature* **393**, 377–381.

Dingledine R, Borges K, Bowie D & Traynelis SF (1999). The glutamate receptor ion channels. *Pharmacol Rev* **51**, 7–61.

Dravid SM, Prakash A & Traynelis SF (2008). Activation of recombinant NR1/NR2C NMDA receptors. *J Physiol* **586**, 4425–4439.

Edwards MA, Loxley RA, Powers-Martin K, Lipski J, McKitrick DJ, Arnolda LF & Phillips JK (2004). Unique levels of expression of N-methyl-D-aspartate receptor subunits and neuronal nitric oxide synthase in the rostral ventrolateral medulla of the spontaneously hypertensive rat. *Brain Res Mol Brain Res* **129**, 33–43.

Farrant M, Feldmeyer D, Takahashi T & Cull-Candy SG (1994). NMDA-receptor channel diversity in the developing cerebellum. *Nature* **368**, 335–339.

Formenti A & De Simoni A (2000). Effects of extracellular Ca^{2+} on membrane and seal resistance in patch-clamped rat thalamic and sensory ganglion neurons. *Neurosci Lett* **279**, 49–52.

Fu Y, Sun W, Shi Y, Shi R & Cheng JX (2009). Glutamate excitotoxicity inflicts paranodal myelin splitting and retraction. *PLoS One* **4**, e6705.

Ishii T, Moriyoshi K, Sugihara H, Sakurada K, Kadotani H, Yokoi M, Akazawa C, Shigemoto R, Mizuno N, Masu M, *et al.* (1993). Molecular characterization of the family of the *N*-methyl-D-aspartate receptor subunits. *J Biol Chem* **268**, 2836–2843.

Káradóttir R & Attwell D (2007). Neurotransmitter receptors in the life and death of oligodendrocytes. *Neuroscience* **145**, 1426–1438.

Káradóttir R, Cavelier P, Bergersen LH & Attwell D (2005). NMDA receptors are expressed in oligodendrocytes and activated in ischaemia. *Nature* **438**, 1162–1166.

Káradóttir R, Hamilton NB, Bakiri Y & Attwell D (2008). Spiking and nonspiking classes of oligodendrocyte precursor glia in CNS white matter. *Nat Neurosci* **11**, 450–456.

Kuner T & Schoepfer R (1996). Multiple structural elements determine subunit specificity of Mg^{2+} block in NMDA receptor channels. *J Neurosci* **16**, 3549–3558.

Kutsuwada T, Kashiwabuchi N, Mori H, Sakimura K, Kushiya E, Araki K, Meguro H, Masaki H, Kumanishi T, Arakawa M, et al. (1992). Molecular diversity of the NMDA receptor channel. *Nature* **358**, 36–41.

Lee JM, Zipfel GJ & Choi DW (1999). The changing landscape of ischaemic brain injury mechanisms. *Nature* **399**, A7–14.

Lipton SA & Rosenberg PA (1994). Excitatory amino acids as a final common pathway for neurologic disorders. *N Engl J Med* **330**, 613–622.

Manning SM, Talos DM, Zhou C, Selip DB, Park HK, Park CJ, Volpe JJ & Jensen FE (2008). NMDA receptor blockade with memantine attenuates white matter injury in a rat model of periventricular leukomalacia. *J Neurosci* **28**, 6670–6678.

Matsuda K, Fletcher M, Kamiya Y & Yuzaki M (2003). Specific assembly with the NMDA receptor 3B subunit controls surface expression and calcium permeability of NMDA receptors. *J Neurosci* **23**, 10064–10073.

Micu I, Jiang Q, Coderre E, Ridsdale A, Zhang L, Woulfe J, Yin X, Trapp BD, McRory JE, Rehak R, Zamponi GW, Wang W & Stys PK (2006). NMDA receptors mediate calcium accumulation in myelin during chemical ischaemia. *Nature* **439**, 988–992.

Monyer H, Burnashev N, Laurie DJ, Sakmann B & Seeburg PH (1994). Developmental and regional expression in the rat brain and functional properties of four NMDA receptors. *Neuron* **12**, 529–540.

Monyer H, Sprengel R, Schoepfer R, Herb A, Higuchi M, Lomeli H, Burnashev N, Sakmann B & Seeburg PH (1992). Heteromeric NMDA receptors: molecular and functional distinction of subtypes. *Science* **256**, 1217–1221.

Neher E & Stevens CF (1977). Conductance fluctuations and ionic pores in membranes. *Ann Rev Biophys Bioeng* **6**, 345–381.

Norton WT & Poduslo SE (1973). Myelination in rat brain: method of myelin isolation. *J Neurochem* **21**, 749–757.

Park E, Velumian AA & Fehlings MG (2004). The role of excitotoxicity in secondary mechanisms of spinal cord injury: a review with an emphasis on the implications for white matter degeneration. *J Neurotrauma* **21**, 754–774.

Pérez-Otaño I, Schulteis CT, Contractor A, Lipton SA, Trimmer JS, Sucher NJ & Heinemann SF (2001). Assembly with the NR1 subunit is required for surface expression of NR3A-containing NMDA receptors. *J Neurosci* **21**, 1228–1237.

Priel A, Gil Z, Moy VT, Magleby KL & Silberberg SD (2007). Ionic requirements for membrane-glass adhesion and giga seal formation in patch-clamp recording. *Biophys J* **92**, 3893–3900.

Salter MG & Fern R (2005). NMDA receptors are expressed in developing oligodendrocyte processes and mediate injury. *Nature* **438**, 1167–1171.

Sasaki YF, Rothe T, Premkumar LS, Das S, Cui J, Talantova MV, Wong HK, Gong X, Chan SF, Zhang D, Nakanishi N, Sucher NJ & Lipton SA (2002). Characterization and comparison of the NR3A subunit of the NMDA receptor in recombinant systems and primary cortical neurons. *J Neurophysiol* **87**, 2052–2063.

Tekkök SB, Ye Z & Ransom BR (2007). Excitotoxic mechanisms of ischemic injury in myelinated white matter. *J Cereb Blood Flow Metab* **27**, 1540–1552.

Tessier-Lavigne M, Attwell D, Mobbs P & Wilson M (1988). Membrane currents in retinal bipolar cells of the axolotl. *J Gen Physiol* **91**, 49–72.

Werner P, Pitt D & Raine CS (2001). Multiple sclerosis: altered glutamate homeostasis in lesions correlates with oligodendrocyte and axonal damage. *Ann Neurol* **50**, 169–180.

Yamakura T, Askalany AR, Petrenko AB, Kohno T, Baba H & Sakimura K (2005). The NR3B subunit does not alter the anesthetic sensitivities of recombinant *N*-methyl-D-aspartate receptors. *Anesth Analg* **100**, 1687–1692.

Ziak D, Chvatal A & Sykova E (1998). Glutamate-, kainate- and NMDA-evoked membrane currents in identified glial cells in rat spinal cord slice. *Physiol Res* **47**, 365–375.

Author contributions

NMDA receptor constructs were made in the Pérez-Otaño lab; all other work was done in the Attwell and Kittler labs. Contributions were as follows. Conception and design of experiments: D.A., V.B., G.F., J.K. Collection, analysis and interpretation of data: D.A., V.B., G.F., J.K., I.P.-O. Drafting the article and revising it: D.A., V.B., G.F., J.K. All authors approved the final submission.

Acknowledgements

This work was supported by the Wellcome Trust, MRC and EU (Leukotreat).